Research of EV's Charging and Discharging Control Considering Demand Response

Huachun Han[1,2], Haiping Xu[1] ,Wei Zhao[1,2], Zengquan Yuan[1]
[1] Key Laboratory of Power Electronics and Electric Drive, Inst. of Electrical Engineering(IEE), Chinese Academy of Science(CAS), China
[2] University of Chinese Academy of Science, China
E-mail: hanhuachun@mail.iee.ac.cn hpxu@mail.iee.ac.cn

Abstract — Large scale of Electric Vehicles(EVs) connected into the power grid will cause a significant impact on distribution network, such as network loss, voltage drop, etc. To solve the problems, this paper proposes a novel control system for EV charge-discharge response to Demand Side. This system adopts an algorithm based on dq0 coordinate transformation to measure grid frequency, adjusts the charge-discharge behaviors of EV dynamically according to the grid status and ultimately realizes EV's charge-discharge process responded to Demand Side. The simulation and experiment verify that the control system can maintain good accuracy and real-time performance.

I. INTRODUCTION

With the increasingly contradiction between economic development and energy supply, environmental pollution, electric vehicles (EVs) are getting more popular as a long term vehicular technology to reduce the dependence on fossil fuel and the emission of greenhouse gases[1].

Large scale of Electric Vehicles (EVs) connected into the Grid will bring ring new opportunities and challenges for the power grid's operation. At present, almost all EVs start charging instantaneously when they are plugged in. Uncoordinated charging has a significant impact on the performance of the grid. One of the most important impacts is the incremental large load caused by PEVs charging [2]. In article [3], the charge capacity of the entire U.S. power grid for EVs is studied, which includes two rechargeable scenes of 24h and 12h. The result shows that the existing U.S. power grid can withstand up to 73% of the EVs load required. The voltage drop, the increasing of power losses [4] and overload of distribution transformers [5] will occur.

Thus, coordinated charging of PEVs is vital for reducing the operation risks and improving the efficiency of power system. The charging and discharging of electric vehicles can be controlled by EV charging infrastructure.

Research on the charging control for large-scale electric vehicles connected in grid has been conducted since as early as the 1980s [6]. Heydt[7] suggest that the charging should coincide with overall peak demand and load management be needed to avoid an overload. EV batteries are considered as flexible loads and assumed to recharge during the night when electricity prices are low and the network is not stressed. The simplest method, time-shifted charging depending on the geographical regions, is proposed in [8]. The charging and discharging of eight plug-in vehicles is optimized where the day-ahead electricity price needed [9]. A price-threshold is proposed to control the charging in [10]. And linear programming also is used to optimal EV's charging. C.Binding[11] adopts linear programming based on price and constraints in the low-voltage distribution grid.

Moreover, the batteries may also be exploited as temporary storage of the fluctuating energy supply, and serve as energy storage resource that can give energy back to the grid while parked. It's known as vehicle-to-grid (V2G) power [12], which can improve the load characteristics of the regional power grid, and realize coordinated development large-scale electric vehicles [13-15].

The paper proposes an EV's charging and discharging control system considering Demand Side. This system's cores are the frequency detection and charge-discharge control module. One is used to detect grid frequency, while the other is to adjust charge-discharge process dynamically.

The content is organized as follows. Section II introduces the overall structure of the charge-discharge control system. In Section III, the frequency detection algorithm is explained in detail, verified by simulation and experiment. Section IV concludes the paper in the end.

II. CHARGE-DISCHARGE CONTROL SYSTEM

Due to the large-scale EVs applications, there is an urgent need for more smart charging management system than existing one that can't meet the requirement of real-time control and demand side management.

Figure 1 shows the system architecture for EV charge-dischage system. The monitor center is used to monitor the charge-discharge control system in this network, and form statistical data obtained through Zigbee communication, due to its stable, reliable, convenient low-cost, self-organization. The power grid offers the electrical energy for EVs and gets energy from EVs when necessary. The proposed charge-discharge control system is mainly used to optimal control the charging and discharging process, with the purpose of response to Demand Side.

The structure diagram of the proposed control system is shown in Fig 2. It includes the voltage detection module, frequency detection module, LCD and Keypad modules, the charge-discharge circuit and communication modules such as CAN, Zigbee and so on.

978-1-4799-5162-8/14/$31.00 ©2014 IEEE

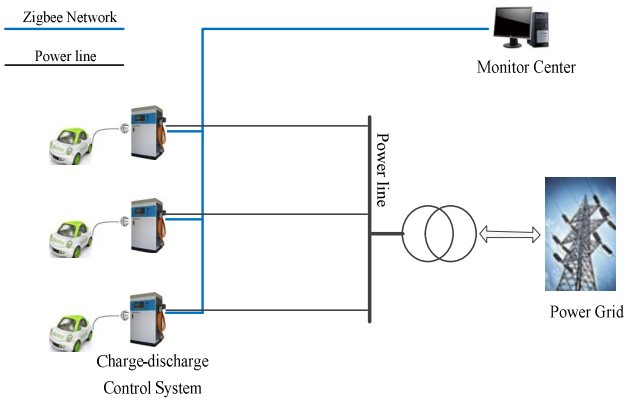

Fig. 1. System architecture for EV charge-dischage system

To realize the EV's charge-discharge process responded to Demand Side, the control system should perceive the status of power grid in real time, and adjust the charging and discharging process of EV's dynamically. And so, the voltage and frequency detection modules are necessary to optimize EV charge-discharge schedules.

The voltage detection module detects the grid voltage value U_{real} at the access point, which is used to be compared with the rated voltage U_0. Then the charge-discharge control system judges the reactive power positive or negative, and controls it release or absorb to maintain a stable grid voltage.

The frequency detection module detects the grid frequency value f_{real} at the access point, which is used to be compared with the rated frequency f_0. Then the charge-discharge control system judges the active power positive or negative, and controls it released or absorbed to maintain a stable grid frequency.

The LCD and Keypad modules are used for users EVs charge information display, and man-machine interface used for drivers' input such as expected duration and so on. The premise of the EV's charging and discharging is to meet the needs of users.

CAN communication module is used for exchanging information between the control system and EV's battery management system(BMS). The real-time battery SOC, battery capacity and other key parameters are obtained by CAN-BUS[16], based on the standard CAN 2.0 communication.

ZigBee wireless communication enables the control system transmit data and control commands with the monitor center. This wire communication may bring many problems such as distance layout and complex route disturbance. So, the wireless
network technology used in electric power automation system is imperative. Due to its stable, reliable, convenient low-cost, self-organization, ZigBee is used to set up the communication network.

The data flow among the proposed charging and discharging, monitor center, user, and BMS is illustrated in Fig.3.

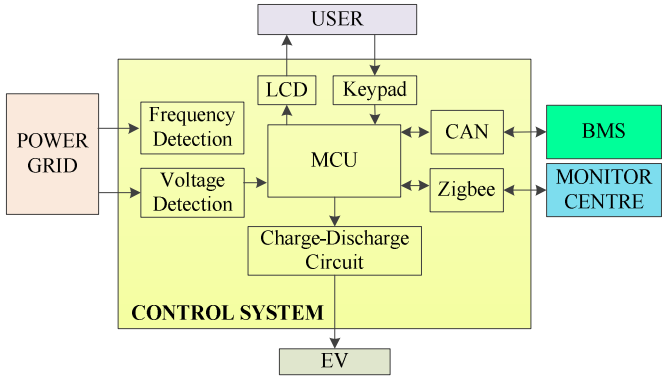

Fig. 2. The structure diagram of EV's charge-discharge control system

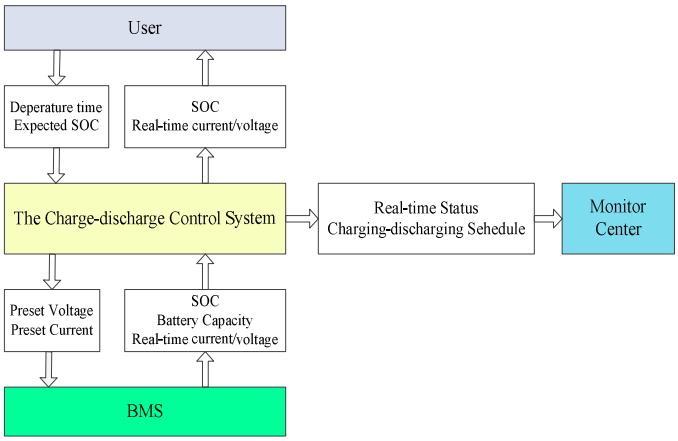

Fig. 3.Schematic for Data Transmission

III. FREQUENCY DETECTION

The frequency detection algorithm is the core technology of the module. Power grid frequency can be obtained by measuring the frequency of voltage or current. Considering the inherent characteristics of the three-phase power grid, the system get the fundamental component through generalized dq0 transform to measure grid frequency[17].

A. Algorithm principle

According to the symmetrical components method, the three-phase voltage can be decomposed into positive, negative and zero sequence components.

$$\begin{cases} u_a = \sum_{n=1}^{\infty} \sqrt{2}[U_n^+ \cos(n\omega t + \varphi_n^+) \\ \quad + U_n^- \cos(n\omega t + \varphi_n^-) + U_n^0 \cos(n\omega t + \varphi_n^0)] \\ u_b = \sum_{n=1}^{\infty} \sqrt{2}[U_n^+ \cos(n\omega t + \varphi_n^+ - 2\pi/3) \\ \quad + U_n^- \cos(n\omega t + \varphi_n^- + 2\pi/3) + U_n^0 \cos(n\omega t + \varphi_n^0)] \\ u_c = \sum_{n=1}^{\infty} \sqrt{2}[U_n^+ \cos(n\omega t + \varphi_n^+ + 2\pi/3) \\ \quad + U_n^- \cos(n\omega t + \varphi_n^- - 2\pi/3) + U_n^0 \cos(n\omega t + \varphi_n^0) \end{cases} \quad (1)$$

Where, u_a , u_b, u_c are the three-phase voltage components, U_n^+, U_n^- , U_n^0, φ_n^+ , φ_n^- , φ_n^0 respectively represent the effective value and initial phase angle of the positive sequence, negative sequence and zero sequence components . n represent n-harmonic, ω for fundamental angular frequency.

$$C_{abc/dq0} = \sqrt{\frac{2}{3}} \begin{bmatrix} \cos\omega t & \cos(\omega t - 2\pi/3) & \cos(\omega t + 2\pi/3) \\ -\sin\theta & -\sin(\omega t - 2\pi/3) & -\sin(\omega t + 2\pi/3) \\ 1/\sqrt{2} & 1/\sqrt{2} & 1/\sqrt{2} \end{bmatrix} \quad (2)$$

According to Park transformation matrix (2), three-phase AC voltage components are transformed into dq0 coordinates, which is shown in Equation (3).

$$\begin{bmatrix} u_d' \\ u_q' \\ u_0 \end{bmatrix} = C_{abc/dq0} \begin{bmatrix} u_a \\ u_b \\ u_c \end{bmatrix} = \begin{bmatrix} \sqrt{3}\sum_{n=1}^{\infty}[U_n^+ \cos((n\omega - \omega_0)t + \varphi_n^+) + U_n^- \cos((n\omega + \omega_0)t + \varphi_n^-)] \\ \sqrt{3}\sum_{n=1}^{\infty}[U_n^+ \sin((n\omega - w_0)t + \varphi_n^+) - U_n^- \cos((n\omega + \omega_0)t + \varphi_n^-)] \\ \sqrt{6}\sum_{n=1}^{\infty} U_n^0 \cos(n\omega t + \varphi_n^0) \end{bmatrix} \quad (3)$$

Where ω_0 is synchronous rotating angular frequency, which equals to 100π.

Equation (3) shows that the fundamental component in three-phase coordinates is transformed into a low-frequency AC component. According to the National standard, the fluctuation range of frequency is limited to ±5Hz. The deference between the lowest frequency of harmonics and the fundamental component is about 50Hz. And it's also close to 50Hz of the difference between fundamental positive sequence components and fundamental negative sequence component after converting.

Thus, as long as setting reasonably such parameters of low-pass filter as the cut-off frequency and attenuation coefficient, the fundamental component can still get through low-pass filter, while harmonics are attenuated as high frequency components. Equation (4) shows the fundamental positive sequence component after filtering.

$$\begin{bmatrix} u_d \\ u_q \end{bmatrix} = \begin{bmatrix} \sqrt{3}U_1^+ \cos((\omega - \omega_0)t + \varphi_1^+) \\ \sqrt{3}U_1^+ \sin((\omega - \omega_0)t + \varphi_1^+) \end{bmatrix} \quad (4)$$

Discretizing signal in (4), there is

$$\begin{bmatrix} u_d(n) \\ u_q(n) \end{bmatrix} = \begin{bmatrix} U_1^+ \cos(2\pi n\Delta t(f_{real} - f_0)t + \varphi_1^+) \\ U_1^+ \sin(2\pi n\Delta t(f_{real} - f_0)t + \varphi_1^+) \end{bmatrix} \quad (5)$$

Where, $u_d(n)$, $u_q(n)$ are the calculating values of n times sample. Δt is the sampling interval time. f_{real} is the actual grid frequency; f_0 is the initial frequency. Considering grid frequency fluctuating in the vicinity of the standard frequency, f_0 is set to be the standard frequency 50Hz.

Combining with trigonometric function formulas, the frequency of power grid can be calculated from Equation (5).

$$f_{real}(n) = \frac{1}{2\pi\Delta t}\left(\arccos\frac{u_d(n)}{\sqrt{u_d(n)^2 + u_q(n)^2}} - \arccos\frac{u_d(n-1)}{\sqrt{u_d(n-1)^2 + u_q(n-1)^2}}\right) + f_0 \quad (6)$$

It's clear that initial phase angle disappeared in the calculation process, which has no effect on this algorithm. The sampling interval can be set, and has small impact on measuring grid frequency. And so, this algorithm has a good real-time performance. The calculation diagram is shown in Fig 4.

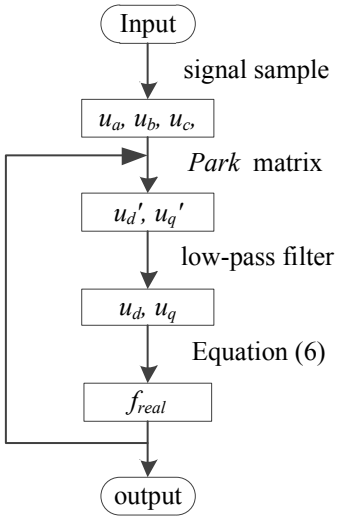

Fig.4. The calculation diagram

B. Anaysis of simulation results

Simulate in MATLAB to verify the accuracy of the algorithm. The actual grid mainly contains odd harmonics, in which 3-times and 5-times harmonic. The input signal source is constructed as follow.

$$\begin{cases} u_a = 220\cos(wt) + 44\cos(3wt) \\ \quad +22\cos(5wt) + \zeta \\ u_b = 220\cos(wt - 2\pi/3) + 44\cos(3wt - 2\pi/3) \\ \quad +22\cos(5wt + 2\pi/3) + \zeta \\ u_c = 220\cos(wt + 2\pi/3) + 44\cos(3wt + 2\pi/3) \\ \quad +22\cos(5wt - 2\pi/3) + \zeta \end{cases} \quad (7)$$

Where ζ is the Gaussian white noise signal with noise ratio 40dB. The Butterworth low-pass filter with a cut-off frequency of 15Hz is adopt. The results are shown in TABLE 1 and Fig 5.

TABLE I
SIMULATED RESULTS OF FREQUENCY MEASUREMENT

Real Frequency (Hz)	50ms		160ms	
	Measuring frequency (Hz)	Relative Err (%)	Measuring frequency (Hz)	Relative Err (%)
45	45.2073	0.4608	44.9803	-0.0437
47	47.0994	0.2114	47.0215	0.0457
48.5	48.5375	0.0774	48.4842	-0.0326
49.4	49.4021	0.0043	49.4105	0.0212
50	49.9774	-0.0453	50.0151	0.0301
50.6	50.5506	-0.0975	50.5972	-0.0056
51.5	51.4059	-0.1826	51.4889	-0.0216
53	52.8230	-0.3340	53.0106	0.02
55	54.7232	-0.5033	55.0011	0.0020

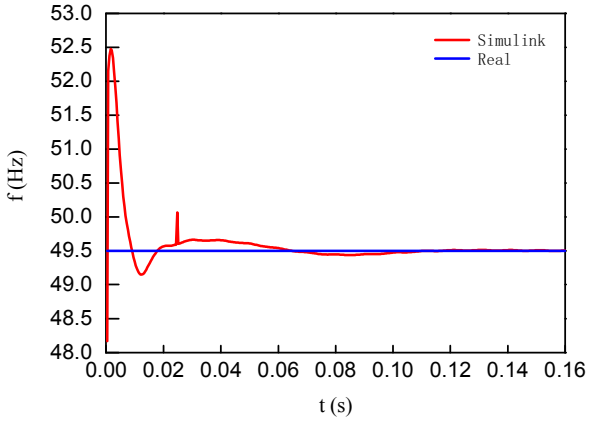

Fig. 5. The graph of frequency tracking process.

From the TABLE II, It's clear that the accuracy of the algorithm is less than 1% at 50ms and less than 0.1% at 160ms. the frequency. Figure 5 shows the frequency tracking process while the real grid frequency is 49.5Hz. At the beginning of system step response, the tracking signal shocks at around 49.5Hz. The shock gets weaker at about 60ms, while the error range is within one-thousandth.

C. *Experimental Verification*

Variable-frequency Drive is used to generate the three-phase voltage signals in (7) in the laboratory environment. The frequency detection module of EV charge-discharge device collects the voltage signals and calculates the value using the algorithm. The test results of the given signals above are listed in the following table I. The main control chip comes from TI MSP430 series.

The data acquisition frequency is set to be 2500Hz. We can obtain the first calculated value until 400 data collected. This process requires only 160ms.

From TABLE II, we can find that this algorithm can be applied to a range of 45-55Hz grid frequency measurement. Even if step response occurred, the frequency value can also be precisely measured grid in 160ms, with relative error less than 1%. The EV charge-discharge device can perceive the status of power grid, and realize the EV's charge-discharge process quickly responded to Demand Side.

TABLE II
EXPERIMENTAL RESULTS OF FREQUENCY MEASUREMENT

Real frequency (Hz)	Measure frequency (Hz)	Err （Hz）	Relative Err (%)
45	45.32	0.32	0.7111
47	47.27	0.27	0.5745
48.5	48.79	0.29	0.5979
49.5	49.11	-0.39	-0.7879
50	50	0	0
50.5	50.95	0.45	0.8911
51.5	51.21	-0.29	-0.5631
53	52.73	-0.27	-0.5094
55	54.68	-0.32	-0.5818

IV. CONCLUSION

In this paper, a novel EV's charging and discharging control system response considering demand side is proposed. Measuring frequency in timely and accuracy is the core technology of the control system. The paper adopts a frequency measure algorithm based on dq0 coordinate transformation. Both simulation and experiment verify that the algorithm can maintain good accuracy and real-time performance over a wide frequency range. The control system can real-time perceive the status of power grid, dynamic adjust the charging and discharging process of EV's, and realize the EV's charge-discharge behavior responded to Demand side.

ACKNOWLEDGMENT

The author would like to thank the fund and support of the National Science Foundation of China, Project no (51077122).

V. REFERENCES

[1] Ouyang Minggao. "Chinese development strategy and countermeasure of energy-saving and new energy automotive," *Automotive Engineering*, Vol. 28, No. 4, pp. 317-321, 2006.

[2] Zhao Junhua, Wen Fushuan, Yang Aimin, et al. "Impacts of electric vehicles on power systems as well as the associated dispatching and control problem," *Automatin of Electric Power Systems,* 2011, 35(14): 2–10, 29 Vol. 35, No.14, pp. 2-10,29, 2006.

[3] Kintner-Meyer, M.C., K.P. Schneider and R.G. Pratt. "Impacts Assessment of Plug-in Hybrid Vehicles on Electric Utilities and Regional US Power Grids: Part1: Technical Analysis," *Online Journal of EUEC.* pp. 1-4. 2007.

[4] Pieltain Fernandez L, Gomez San Roman T et al. "Assessment of the Impact of Plug-in Electric Vehicles on Distribution Networks," *IEEE Trans. Power Systems,* Vol. 26, pp. 206-213, May. 2011.

[5] Staats P T, Grady W M, Arapostathis A and Thallam R S. "A procedure for derating a substation transformer in the presence of widespread
[6] S. Rahman and G. B. Shrestha, "An investigation into the impact of electric vehicle load on the electric utility distribution system," *IEEE Trans. Power Del*., Vol. 8, no. 2, pp. 591–597, Apr. 1993.
[7] G. T. Heydt, "The impact of electric vehicle deployment on load management strategies," *IEEE Trans. Power App. Syst.*, Vol. PAS-102, no.5, pp. 1253–1259, May 1983.
[8] F. Koyanagi and Y. Uriu, "A strategy of load leveling by charging and discharging time control of electric vehicles," *IEEE Trans. Power Syst,* Vol. 13, no. 3, pp. 1179–1184, 1998.
[9] G. K. Venayagamoorthy, P. Mitra, K. Corzine, and C.Huston, "Real-time modeling of distributed plug-in vehicles for V2G transactions," *in Proc. IEEE Energy Convers. Congr. Expo., San Jose*, pp. 3937–3941. Sep. 2009.
[10] E. Larsen, D. K. Chandrashekhara, and J. Oestergaard, "Electric vehicles for improved operation of power systems with high wind power penetration," *in Proc. IEEE Energy 2030 Conf.*, Atlanta, GA, pp. 1–6. Nov 2008.
[11] O.Sundström and C.Binding, "Planning Electric-Drive Vehicle Charging Under Constrained Grid Conditions," *IBM Research Report-Zurich, Switerland*, Aug 2010.
electric vehicle battery charging," *IEEE Trans. Power Delivery*, Vol. 12, pp. 1562-1568, Aug. 2008.
[12] Gao Ciwei, Zhang Liang. "A survey of influence of electrics vehicle charging on power grid," *Power System Technology*, Vol. 35, no.3, pp.127-131, 2011.
[13] Singh M, Kar I, Kumar P. " Influence of EV on grid power quality and optimizing the charging schedule to mitigate voltage imbalance and reduce power loss," *Power Electronics and Motion Control Conference. Ohrid:* IEEE, pp.196-203, 2010.
[14] KEMP TON W, LETENDRE S. "Electric vehicles as a new power source for electric utilities," *Transportation Research: Part D*, Vol. 2, no. 3, pp. 157-175, 1997.
[15] Ma Yuchao, Tom Houghton, Andrew C, et al. "Modeling the benefits of vehicle-to-grid technology to a power system," *IEEE Trans on Power Systems,* Vol. 27, no.2, pp.1012-1020,2012.
[16] Xiao-feng Wan, Yi-si Xing, Li-xiang Cai. "Application and implementation of CAN bus technology in industry real-time data communication," *Industrial Mechatronics and Automation*, pp. 278-281, May 15-16, 2009.
[17] Yin Haiwen, Mu Longhua. "A frequency measuring algorithm based on d-q-0 transformation," *Power System Protection and Control,* Vol. 39, no.12, pp. 79-83, 2011.